532.135:678.027

A Study of Viscoelastic Fluid Flow*

(2nd Report, Extrudate Irregularities)

By Yukio TOMITA** and Ken TSUCHIYA***

In the flow of molten high polymers through capillaries, an instability occurs at shear stresses $10^6 \sim 10^8$ dynes/cm^2. The instability results in emerging streams of irregular shape. Several explanations of extrudate irregularities have been published up to the present, but they may be considered to be insufficient.

In this paper, considering that the flow states of a viscoelastic fluid are governed by the elastic force, the viscous force and the inertia force, two dimensionless numbers R_e* and N_E are deduced. Then, it is verified by the experiment that the onset of instabilities in an extrudate of molten high polymers depends on these dimensionless numbers R_e* and N_E.

1. Introduction

In the flow of molten high polymers through capillaries, an instability occurs at shear stresses 10^6 to 10^8 dynes/cm^2 [1], that is, phenomena such as ripple mark and crack on the extrudate surface are brought about. This irregularity causes a deterioration of extrudate's mechanical properties and restricts the productivity by extruding process. Therefore, many studies have been made on the cause of its occurrence, but no established theory has been presented up to now[2].

Westover and Maxwell[3] have considered that the turbulence of a flow in a capillary is the cause of instability, and the flow becomes irregular when Reynolds number R_e defined as below has some constant value.

$$R_e = \frac{\rho u_a r_0}{\mu} = \frac{\rho Q}{\pi r_0 \mu} \quad \cdots\cdots(1)$$

where u_a is the average flow velocity in the capillary; ρ is the density of melt; r_0 is the inner radius of capillary; μ is the apparent viscosity of melt and Q is the flow rate. Metzner[2], however, objects to this remark because the estimation of Reynolds number at the onset of instabilities becomes below 10^{-4}. Also, assuming that R_e=constant at the critical point, when μ=constant, Q is proportional to r_0^3 according to the Tordella's experiment[4], but proportional to r_0 in Eq. (1); and when r_0=constant, Q is inversly proportional to μ, but proportional to μ in Eq. (1). From these view-points, Westover and Maxwell's opinions may not be able to be accepted.

Spencer and Dillon[5] have considered that the occurrence of surface irregularity results from the interaction between the outer layer about the capillary wall which is stretched and is going to recover elastically, and the inner layer about the central axis which is not stretched. Philippoff[6] has maintained that the cause of instability is the normal stress which is a longitudinal tensile stress in the fluid flowing through a capillary. These several explanations of extrudate irregularity show that the origin of instability is in the exit or the interior of capillary. Tordella[4], however, pointed out that the flow state at the inlet to the capillary plays an important part in the irregular phenomenon. Tordella observed the state of flow at the capillary inlet when the irregularities occurred, and he found a disordered flow pattern. He, therefore, proposed the following new dimensionless number as opposed to Reynolds number as the parameter with which to predict the onset of fracture:

$$N_J = \frac{\mu u_a J}{r_0} = \frac{\mu Q J}{\pi r_0^3} \quad \cdots\cdots(2)$$

where J is a compliance and equal to the reciprocal of modulus of elasticity. With Eq. (2), the experimental results can be explained, that is to say, if N_J=constant, Q is in reciprocal proportion to μ and proportional to r_0^3. But the reciprocal relation between Q and J in Eq. (2) may not be consistent with experimental results. Then, Metzner and other's[7] experimental results (cf. Table 3) that the critical shear rate at which irregularities begin is dependent on the ratio of capillary length to radius,

* Received 16th July, 1962.
** Assistant Professor, Tokyo Institute of Technology, Meguro-ku, Tokyo.
*** Research Engineer, Japan Steel Works, Ltd.

l/r_0, are not explained, and they showed that the value of N_J at the critical state varied with different melts, although, of course, their estimate for N_J may be open to discussion.

Moreover, Spencer[8] has found out the fact through the experiments over a wide range of temperature with polystyrene that the critical shear rate is in reciprocal proportion to the relaxation time, and Clegg[9] has determined the apparent relaxation time of polyethylenes with different degrees of branching and obtained the results that the critical shear rate decreases with an increasing relaxation time.

In this paper, the factors which govern the flow of polymer melts are examined, and the dimensionless numbers for determining the limit at which the irregularity begins are introduced. Then, it is shown by the experiments that the onset of instabilities in an extrudate of molten high polymers depends on these dimensionless numbers.

2. Pressure drop due to elasticity at capillary inlet

When a viscoelastic fluid such as polymer melts flows into a capillary from a large cistern, pressure drop occurs on many occasions. If the velocity is small and the contraction of a flow does not occur at the capillary entry and a steady flow is directly obtained there, that is, the inlet length is nearly zero, it is considered that the so-called additional entrance loss is the sum of the energy dissipated by viscosity and the elastic energy stored in the fluid while the fluid reaches the capillary entrance from the large cistern. Assuming that the strain component caused in the viscoelastic fluid is an m-th power proportional to the corresponding component of rate-of-strain, namely

$$\varepsilon_{ij}=\lambda e_{ij}^{m} \quad \cdots\cdots(3)$$

(ε_{ij}: a component of the strain tensor, e_{ij}: a component of the rate-of-strain tensor, λ: the proportional constant), one of the authors analyzed approximately an inflow from the plane wall to the capillary, and expressed the elastic energy I_E stored per unit time throughout the flowing fluid in the following expression[10]:

$$I_E=KGQD^{2m} \quad \cdots\cdots(4)$$

where G is the modulus of rigidity, $D=(4Q)/(\pi r_0^3)$ is the apparent shear rate in the capillary, and K is expressed as follows:

$$\left.\begin{aligned} K&=\lambda^2 K' \\ K'&=\frac{1}{4^{2m}}\left\{\frac{A'}{2}+\frac{mA''}{n(2m+1)+3}-\frac{mB''}{2(mn+1)}\right\}\end{aligned}\right\} \quad \cdots\cdots(5)$$

$$A'=\int_0^{\pi/2}\{2^{2m+1}(2^{2m-1}+1)\cos^{2m+1}\theta+2\sin^{2m}\theta\cos\theta\}\sin\theta d\theta \quad \cdots\cdots(6)$$

$$\begin{aligned} A''=\int_0^{\pi/2}\Bigg[&\frac{2^{2(m+1)}}{(n+1)}\left\{2^{2m-1}+1\right\}\cos^{2m+1}\theta+2(n+3)\left\{2n(n+3)^{2m-1}+\frac{(n+2)^{2m}}{(n+1)}\right\}\sin^{2m}\theta\cos\theta \\ &+\frac{2^{2m+1}(n+3)}{(n+1)}\left\{2^{2m-1}+1\right\}\cos^{2m-1}\theta\sin^2\theta\Bigg]\sin\theta d\theta \end{aligned} \quad \cdots\cdots(7)$$

$$\begin{aligned} B''=\int_0^{\pi/2}\Bigg[&\frac{2^{2m+1}(n+3)}{(n+1)}\left\{2^{2m-1}+1\right\}\cos^{2m+1}\theta+2(n+2)^{2m}(n+3)\sin^{2m}\theta\cos\theta \\ &+\frac{3\times 2^{2m}(n+3)}{(n+1)}\cos^{2m-1}\theta\sin^2\theta\Bigg]\sin\theta d\theta \end{aligned} \quad \cdots\cdots(8)$$

also n is a rheological constant, that is, the exponent in the power-law characterizing the flow property of a non-Newtonian fluid. For example, Fig. 1 shows the calculated values of K' corresponding to n when $m=0.5$. Applying the theory of elasticity of large deformation to the steady simple shear flow of a viscoelastic fluid, m, λ and G will be found experimentally[11], and the elastic energy stored per unit time may be determined from Eqs. (4) and (5). (Although Eq. (3) and power-law of non-Newtonian viscosity may not be applied over a wide range of shear rate, they will be able to explain the viscoelastic phenomena in a limited range of shear rate. Moreover, as Eq. (4) is the result based on the theory of elasticity of small deformation, there is a doubt about the application of m, λ and G which are obtained based on the theory of elasticity of large deformation. Concerning these problems, we shall study in future.)

Now, putting the pressure drop due to elasticity at the entry of capillary as Δp_E, the following relation is obtained:

$$I_E=\Delta p_E Q \quad \cdots\cdots(9)$$

and from Eqs. (4) and (9) we have

$$\Delta p_E=KGD^{2m} \quad \cdots\cdots(10)$$

Fig. 2 shows the result of experiment with high-density polyethylene melt ($t=240°C$, $n=2.73$, $\mu_{psu}=8.77\times10^{13}$ g^n/cm^n·sec^{2n-1}). Δp_E in this figure is obtained by deducting the pressure drop Δp_V due to viscosity from the measured value of pressure drop Δp, in the manner explained in the 1st report. It is shown that putting $m=0.39$ in Eq. (10), the above experimental data are found on the line expressed by $\Delta p_E=KGD^{0.78}$ and KG becomes 1.27×10^5 g/cm·sec$^{2(1-m)}$. Although Eq. (10) is the relation introduced for the case where the entry of capillary is flat and the inlet length neglected, we suppose that Eq. (10) may approximately hold even if these conditions are not satisfied. In such a case, K in Eq. (10) will change not only with n and m, but also with the entry shape of a capillary and the velocity distribution at the capillary entrance. Fig. 3 shows, as an example, the result of experiment made with the entry taper nozzle (material: low-density polyethylene, $t=250°C$, $n=1.64$, $\mu_{psu}=3.56\times10^6$ g^n/cm^n·sec^{2n-1}). Putting $m=0.63$ in Eq. (10), the results are described in $\Delta p_E=1.89\times10^3 D^{1.26}$. Comparing with other experimental results made with different taper nozzles, it is found that Eq. (10) may approximately be applicable to various types of nozzles. (There is slight obscurity about the estimation of pressure drop Δp_V due to viscosity. However, it will not cause any trouble because Δp_V is very small comparing with Δp_E if the entry angle of nozzle is not too small.) It has been reported that in extrusion of molten plastics with a screw extruder, the uniformity of product's quality could be improved by increasing the mixing and kneading, and equalizing the state of flow by raising the pressure at the tip of the screw (back pressure). Thus, there is the back pressure control method[12] to make the back pressure higher by inserting a resistance such as a screen pack, a fixed orifice and a valve, between the tip of screw and the die. Maddock[13] considered that the relation between the flow rate Q and the pressure drop Δp through the fixed orifice as shown in Fig. 4, was given by the following expression:

$$\Delta p=\Lambda\mu Q \quad \cdots\cdots(11)$$

and for the circular orifice Λ becomes

$$\Lambda=\frac{128(l+4d)}{\pi d^4} \quad \cdots\cdots(12)$$

where μ is the viscosity, l is the length of orifice and d is the diameter of orifice. Eqs. (11) and (12)

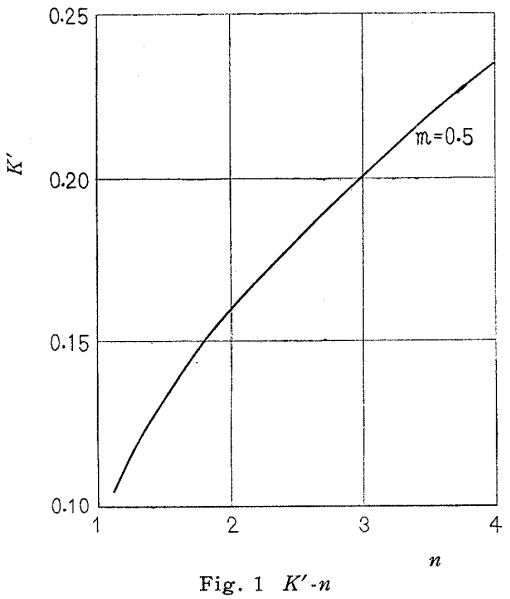

Fig. 1 K'-n

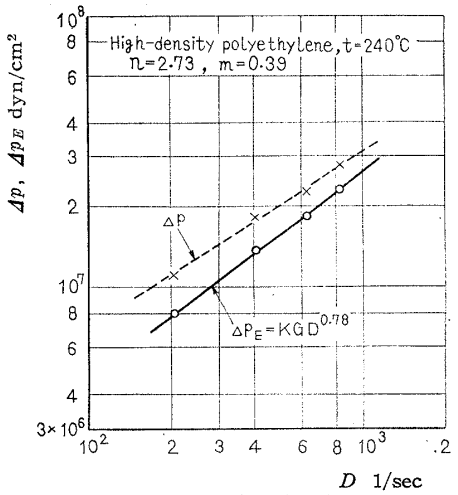

Fig. 2 Δp, Δp_E-D

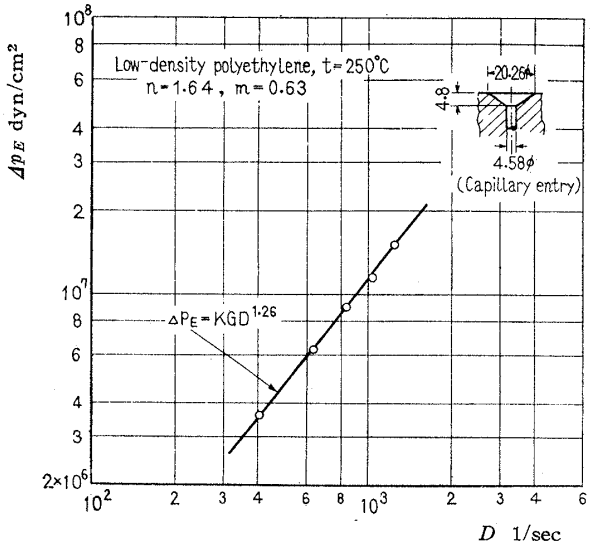

Fig. 3 Δp_E-D, Shape of capillary entry

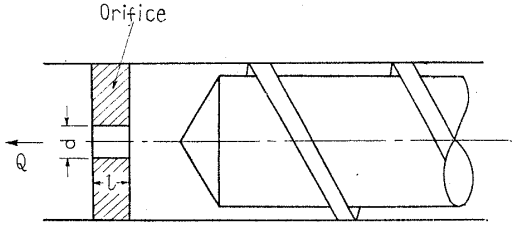

Fig. 4 Orifice

are obtained by replacing the length of orifice l in the Hagen-Poiseuille's equation by $(l+4d)$ adding $4d$ as the end correction. But, as mentioned previously, molten plastics show remarkable elasticity, and the end correction is a strong function of the apparent shear rate. It is therefore considered to be adequate that the relation between the pressure drop and the flow rate is expressed as follows:

$$\Delta p=\Theta(\mu_{psu}Q)^{1/n} \quad \cdots\cdots(13)$$

and Θ is

$$\Theta=\left\{\frac{2^{2n+3}(n+3)}{\pi d^{n+3}}\right\}^{1/n}\left[l+\left\{\varepsilon_V+\frac{K}{4^{(n-1)/n}(n+3)^{1/n}}\frac{G}{\mu_{psu}{}^{1/n}}D^{(2mn-1)/n}\right\}d\right] \quad \cdots\cdots(14)$$

where μ_{psu} and n are rheological constants concerning the viscosity and defined with Eq. (19). Also, ε_V is the function of n as shown in Fig. 5[14]. Thereby, if n, μ_{psu}, m and KG are previously obtained about various molten plastics, the relation between the pressure drop Δp and the flow rate Q may be found more precisely with Eqs. (13) and (14) than with Eqs. (11) and (12).

3. Dimensionless parameters governing viscoelastic fluid flow

If the factors governing the flow state of a viscoelastic fluid as polymer melt are ascertained, whatever may be the cause of the irregularity, the terms for the instability flow stale being continued, that is, the dimensionless parameters prescribing the onset of instability may be obtained. Assuming that the viscoelastic fluid which is here treated possesses the elasticity of shape only and the volume is invariable, the forces acting on the fluid will be three kinds, that is, the elastic force, the viscous force and the inertia force. Then, the flow state may be governed by any two ratios in the following ratios of the forces or the stresses:

$$\left.\begin{array}{lll}\dfrac{\text{the inertia force}}{\text{the viscous force}}, & \dfrac{\text{the inertia force}}{\text{the elastic force}}, & \dfrac{\text{the elastic force}}{\text{the viscous force}}\\ \text{or} & & \\ \dfrac{\text{the pressure}}{\text{the viscous stress}}, & \dfrac{\text{the pressure}}{\text{the elastic stress}}, & \dfrac{\text{the elastic stress}}{\text{the viscous stress}}\end{array}\right\} \quad \cdots\cdots(15)$$

Here, the two ratios, that is, (pressure)/(viscous stress) and (elastic stress)/(viscous stress) are taken up for elaborate discussion.

Now, although any theory has not yet been established about the elastic stress originated in the viscoelastic fluid, we analyze under the consideration as follows: that is, as the result of the elastic energy being stored in the fluid up to the capillary entry as explained in the previous section, it is considered that the pressure Δp_E required for extruding the fluid into the capillary may appear as the mean elastic stress σ_E' in the fluid at the capillary entry. (Though this elastic stress may be a normal stress, the stress distribution in the fluid must be discussed more minutely.) Then, from Eq. (10) the mean elastic stress σ_E' may be represented as follows:

$$\sigma_E'=KG\left(\frac{4u_a}{r_0}\right)^{2m} \quad \cdots\cdots(16)$$

As explained previously, K in Eq. (16) varies with n, m and the shape of capillary entrance. Moreover, we consider that this elastic stress σ_E' decreases in a relaxation phenomenon with an increase in the stay-time of the fluid in the capillary. This stress relaxation is expressed as $e^{-t/\kappa'}$ in the Maxwell's model (t: elapsed time, κ': relaxation time); we, however, assume that it is represented as $(\kappa/t)^\alpha$ in which α and $\kappa(<\kappa')$ are constants determined from experiments. Although, in such an expression, a irrationality occurs at $t=0$, we adopt it because the mechanical behaviors of a viscoelastic fluid may perfectly not be represented by the simple Maxwell's model and its brief mathematical treatment. Then, the mean elastic stress σ_E may be presented as follows:

$$\sigma_E=KG\left(\frac{4u_a}{r_0}\right)^{2m}\left(\frac{\kappa}{t}\right)^{\alpha} \quad \cdots\cdots(17)$$

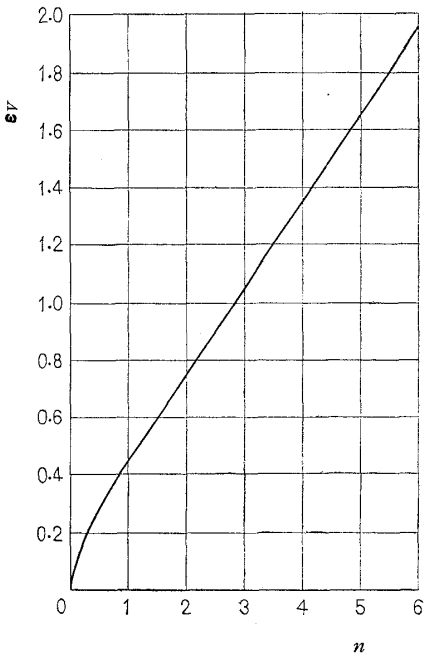

Fig. 5 ε_V-n

Putting $t=l/u_a$ (t: stay-time in capillary, l: length of capillary), Eq. (17) becomes

$$\sigma_E=\frac{4^{2m}KG\kappa^{\alpha}u_a^{2m}}{r_0^{2m}l^{\alpha}} \quad \cdots\cdots(18)$$

On one hand, we assume that for the viscous stress τ_V the de Waele-Ostwald's power-law

$$\tau_V=\mu_{psu}{}^{1/n}\left(\frac{du}{dr}\right)^{1/n} \quad \cdots\cdots(19)$$

is applicable, where μ_{psu} is a similar quantity to the viscosity of a Newtonian fluid and its dimension is $[g^n/cm^n\cdot sec^{2n-1}]$, and the power index n is the constant determined by material and temperature. Here, if the stresses ratio is made using the following expression as the viscous stress,

$$\tau_V \propto \mu_{psu}{}^{1/n}\left(\frac{u_a}{r_0}\right)^{1/n}$$

the flow state is varied not only with the stresses ratio, but also with n. Then, to eliminate this difficulty, assuming that the velocity distribution of a steady flow in the capillary is approximately expressed as

$$u=\frac{(n+3)}{(n+1)}u_a\left\{1-\left(\frac{r}{r_0}\right)^{n+1}\right\} \quad \cdots\cdots(20)$$

we use the mean viscous stress τ_V', that is

$$\tau_V'=\frac{1}{\pi r_0{}^2}\int_0^{r_0}2\pi r\tau_V dr \quad \cdots\cdots(21)$$

Substituting Eqs. (19) and (20) into Eq. (21), we have

$$\tau_V'=\frac{2}{3}(n+3)^{1/n}\mu_{psu}{}^{1/n}\left(\frac{u_a}{r_0}\right)^{1/n} \quad \cdots\cdots(22)$$

Also, as the inertia force p_I per unit area is corresponding to the pressure, it may be represented in the following form:

$$p_I=\frac{1}{2}\rho u_a{}^2 \quad \cdots\cdots(23)$$

But considering that p_I changes with n in the same way as the viscous stress, we use the mean pressure p_I', that is

$$p_I'=\frac{1}{\pi r_0{}^2}\int_0^{r_0}2\pi r\left(\frac{1}{2}\rho u^2\right)dr \quad \cdots\cdots(24)$$

where ρ is the density of fluid. Substituting Eq. (20) into Eq. (24), the following expression is obtained.

$$p_I'=\frac{(n+3)}{2(n+2)}\rho u_a{}^2 \quad \cdots\cdots(25)$$

Consequently, using Eqs. (22) and (25), Eq. (15) becomes

$$R_e^*=\frac{\text{the pressure}}{\text{the viscous stress}}=\frac{\dfrac{(n+3)}{2(n+2)}\rho u_a{}^2}{\dfrac{2}{3}(n+3)^{1/n}\mu_{psu}{}^{1/n}\left(\dfrac{u_a}{r_0}\right)^{1/n}}=\frac{3(n+3)^{1-(1/n)}}{4(n+2)}\frac{\rho u_a{}^{2-(1/n)}r_0{}^{1/n}}{\mu_{psu}{}^{1/n}}$$

Moreover, to make R_e^* accord with the Reynolds number when $n=1$, we change the numerical coefficients a little. Then R_e^* becomes

$$R_e^*=\frac{3(n+3)^{1-(1/n)}}{(n+2)}\frac{\rho u_a{}^{2-(1/n)}r_0{}^{1/n}}{\mu_{psu}{}^{1/n}} \quad \cdots\cdots(26)$$

On the other hand, using Eqs. (18) and (22), Eq. (15) becomes

$$N_E=\frac{\text{the elastic stress}}{\text{the viscous stress}}=\frac{(4^{2m}KG\kappa^{\alpha}u_a{}^{2m})/(r_0{}^{2m}l^{\alpha})}{\dfrac{2}{3}(n+3)^{1/n}\mu_{psu}{}^{1/n}\left(\dfrac{u_a}{r_0}\right)^{1/n}}$$

Moreover, changing the numerical coefficients, N_E becomes

$$N_E=\frac{4^{1+(1/n)-\alpha}KG\kappa^{\alpha}}{(n+3)^{1/n}}\frac{D^{(2m+\alpha)-(1/n)}}{\mu_{psu}{}^{1/n}}\left(\frac{r_0}{l}\right)^{\alpha} \quad \cdots\cdots(27)$$

where $D=(4Q)/(\pi r_0{}^3)$ expresses the apparent shear rate. Putting $n=1$ in Eq. (26), Eq. (1) is obtained, and putting $n=K=1$, $m=\alpha=0$ in Eq. (27), Eq. (2), that is, $N_J=1/N_E$ is obtained. Therefore, it appears that the flow state of viscoelastic fluids in the capillary is governed by the two dimensionless numbers R_e^* and N_E which are represented in Eqs. (26) and (27), respectively. Thus, to examine the limit at which an irregular phenomenon occurs, it is necessary to consider both of R_e^* and N_E at same time. That is to say, the occurrence of irregularities is concerned with the flow states at the inflow zone and in the capillary. Therefore, the flow state at the capillary entry becomes irregular by correlation among the viscous force, the elastic force and the inertia force, and even in the case where an extrudate irregularity occurs if the length of capillary is short; when the length of capillary is sufficiently long, the instability of flow will be suppressed by the relaxation of the elastic force and the viscous force in the capillary, and an extrudate irregularity may not occur. Namely, when the capillary is long, the apparent shear rate D_c at which the irregularity occurs may have a large value.

4. Experimental equipment and method

Used materials are high-density polyethylene (Phillips method, Sholex 5003) and polypropylene (made by AviSun Corp., molecular weight: 130 000).

As the equipment to melt and extrude the materials, Koka Flow Tester (made by Shimazu Seisakusho Co.) was used. The principal part of equipment is shown in Fig. 6. Nozzles used are made of stainless steel and are capillaries with a flat entry. Nozzles' dimensions and ratio of length to diameter are listed together with those used in the Metzner and other's[7] experiment in Table 1. Heating and melting of materials were done with a nichrome wire resistance. Molten materials were extruded after they were kept in a range of ± 0.5°C to experimental temperature for about 10 minutes.

Pressure acting on the plunger was obtained by magnifying the weight through a lever. Extruding output Q cm³/sec was calculated from the diagram on which the relation of downward travel of plunger vs. time was automatically recorded. The state of extrusion was observed through the mirror installed below the nozzle, and when an irregular phenomenon occurred, the critical points were confirmed with repeated experiments. The examples of photographs of the flow state causing an instability are shown in Fig. 7.

Now, the methods for obtaining the various constants included in Eqs. (26) and (27) are as follows:

(i) n and μ_{psu}:

Assuming Eq. (19) on the non-Newtonian viscosity, the relation between the extruding pressure p and the flow rate Q in the case of extruding into the capillary which has length l and radius r_0 from the vessel (cistern) is represented as follows:

$$\log\left(\frac{4Q}{\pi r_0^3}\right)=n\log\left(\frac{r_0 p}{2l}\right)+\log\left\{\frac{4}{(n+3)\mu_{psu}}\right\} \quad \cdots\cdots\cdots\cdots(28)$$

Therefore, the relation between $D=(4Q)/(\pi r_0^3)$ and $\tau_{wa}=(r_0 p)/(2l)$ may be represented by a straight line on the logarithmic diagram, and n is found from the gradient of this straight line. But, as the pressure p includes the additional entrance loss Δp_T, when τ_{wa} and D obtained from capillaries with different values of l/r_0 are plotted on the logarithmic diagram, the larger the value of l/r_0 is, the more the straight line shifts to left-upper direction as shown in Fig. 8. To obtain the correct shear stress τ_w at the wall, one must estimate the value of Δp_T and deduct it from p. Here, we calculated the pressure drop $(p-\Delta p_T)$ due to viscous resistance in straight tube according to the Bagley's method. That is, as shown in Fig. 9, some straight lines are obtained by

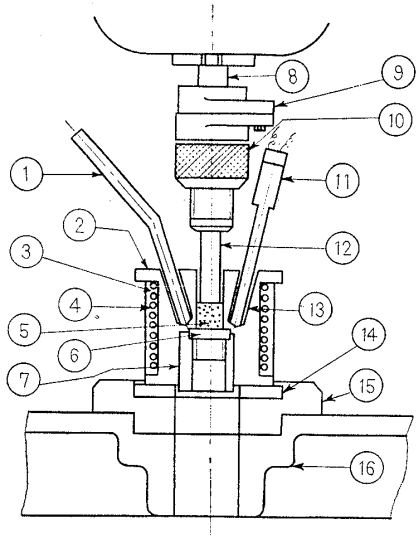

① Mercury thermometer
② Heating cylinder
③ Asbestos (thermal insulator)
④ Nichrome wire
⑤ Test specimen
⑥ Die (nozzle)
⑦ Die tightening screw
⑧ Travelling rod
⑨ Press joint
⑩ Travelling screw
⑪ Thermo-detector
⑫ Plunger
⑬ Wood's metal
⑭ Micalex (thermal insulator)
⑮ Removable base plate
⑯ Base plate

Fig. 6 Principal part of experimental equipment

Table 1 Dimensions of capillaries

Capillary	No. 1	No. 2	No. 3	No. 4	No. 5	No. 6
l/r_0	10.0	20.0	20.0	33.4	40.0	56.0
$d=2r_0$ mm	1.0	1.0	2.0	0.3	1.0	0.5

Capillary	A	B	C	D	E	F	G	H
l/r_0	21.0	27.4	99.4	107.6	109.6	113.0	198.0	264.0
$d=2r_0$ mm	1.20	0.594	1.20	2.29	1.46	0.594	1.20	0.594

(A.B. Metzner et al.[7])

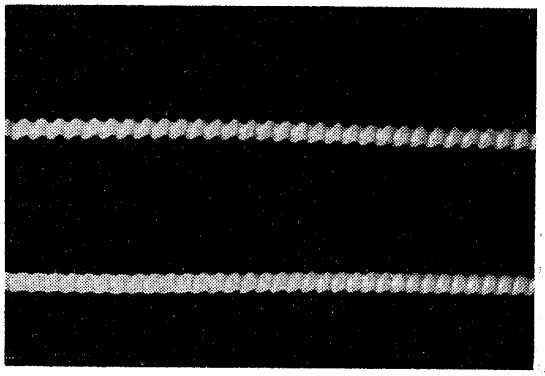

High-density polyethylene, Capillary No.1
Temperature 160°C
Flow direction is right from left on photograph

Fig. 7 Example of occurrence of extrudate irregularities

plotting the relation of p vs. l/r_0 with D as parameter. Making an extrapolation of these lines to the left side, we find p at $l/r_0=0$ equal to the additional entrance loss Δp_T, and intersecting points of the lines and the abscissa give the values of the coefficient of correction ν of the tube length. Then, using

$$\tau_w = \frac{pr_0}{2(l+\nu r_0)}$$

instead of τ_{wa}, D-τ_w relations for capillaries with different values of l/r_0 become the one straight line as shown in Fig. 8, and the gradient of this line gives the correct value of n. Also, μ_{psu} is obtained from the following expression:

$$\mu_{psu} = \frac{4}{n+3}\frac{\tau_w^n}{D} \quad \cdots\cdots(29)$$

(ii) m and KG:

m and KG are calculated by the same method

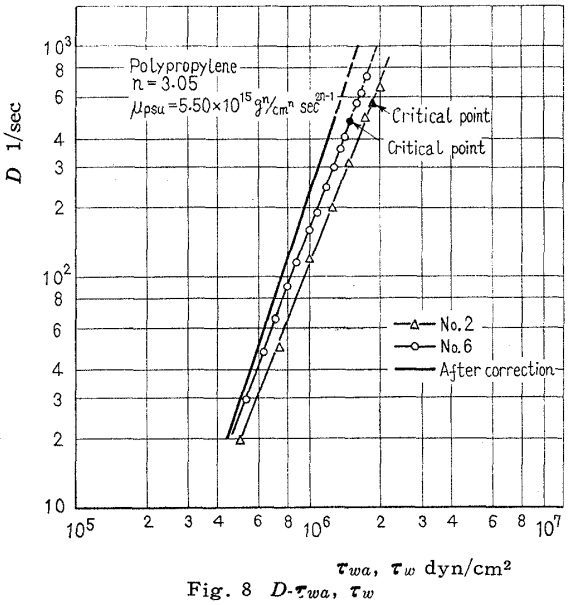

Fig. 8 D-τ_{wa}, τ_w

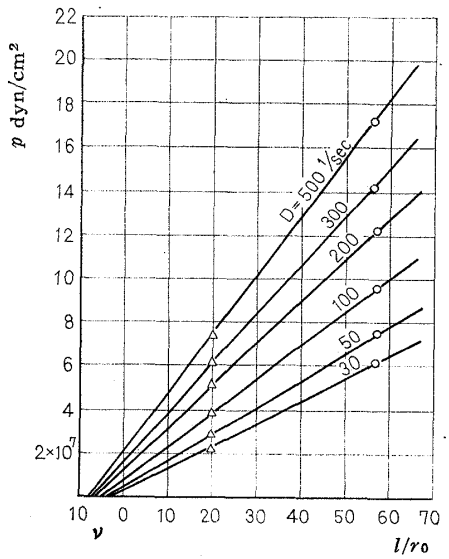

Fig. 9 p-l/r_0, ν

that was used in the section 2. As an example, the experimental result of polypropylene is shown in Fig. 10.

(iii) α and κ:

As the phenomena of stress relaxation in the flowing viscoelastic fluids were not solved theoretically and experimentally up to now, no definite data to be here used on the stress relaxations can be presented. Then, using the following expression obtained from Eq. (27)

$$D \propto \left(\frac{l}{r_0}\right)^{\alpha/\{2m+\alpha-(1/n)\}}$$

α is found, that is, plotting the critical apparent shear rate D_c to l/r_0 on the logarithmic diagram, α may be calculated from the gradient of the obtained straight line because n and m are known. As the effect of l/r_0 on D_c is not distinctly discerned in our experiments in which l/r_0 is comparatively small, assuming that the gradient of straight line is not too much different with different materials and temperatures, α is estimated from the above Metzner and others' experimental data. Although this assumption is groundless, it may not cause any trouble because α will considerably be small.

Also, as the relaxation time κ' of molten polymers is not understood definitely, experimental values of relaxation time of polyethylene have been reported to be 30 to 600 sec[8][9][15] or much larger[16] than these values. However, $\kappa(<\kappa')$ has an effect on N_E as κ^α in Eq. (27) and the value of α is of the order 0.1, therefore, it is considered that the value of N_E will not be too much affected by κ. Namely, κ^α will become nearly 1, but in this report we arrange the experimental results with N_E/κ^α (of course, this is not dimensionless) instead of N_E. In addition, to supplement our data and to compare with our results, the above Metzner and others' results concerning low-density polyethylene are arranged.

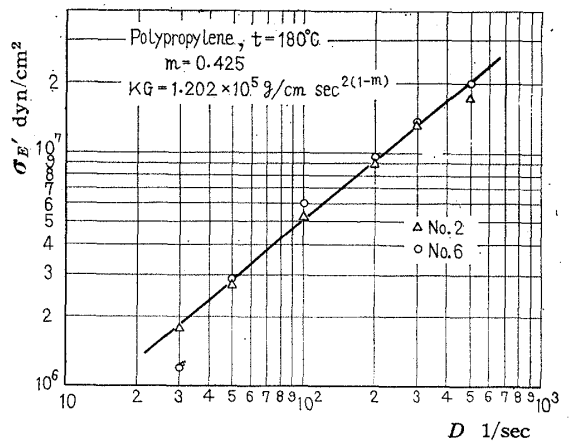

Fig. 10 σ_E'-D

5. Experimental results and discussion

The values of constants are listed in Table 2 and the critical shear rates D_c at which irregular phenomena begin are shown in Table 3. The values of R_e* (Eq. 26) and N_E/κ^α (Eq. 27) calculated using these data are shown in Table 4 and Fig. 11. The critical shear rates range from 2.60×10 to 5.8×10^2 1/sec with materials, temperatures and nozzles. Thus, as shown in Fig. 11, the Reynolds number in a wider sense R_e* at the critical points expands in a markedly wide range from 2.08×10^{-7} to 1.67×10^{-4}, and it is apparent that Westover and Maxwell's theory mentioned above can not be adopted. On the contrary, N_E/κ^α at the critical points is in the range from 4.28×10 to 8.34×10, that is, passably narrow. Thus, it is shown that the ratio of the elastic force to the viscous force is dominant at the parameter deciding whether irregular phenomena occur or not.

Table 2 Various constants

Material	Temperature °C	n	μ_{psu} g^n/cm^n·sec^{2n-1}	ρ g/cm^3	m	KG g/cm·sec$^{2(1-m)}$	α
Polypropylene	180	3.05	5.50×10^{15}	0.76*	0.425	1.02×10^5	0.100
High-density polyethylene	160	2.86	1.47×10^{15}	0.765	0.300	7.83×10^5	0.125
	180	2.62	4.06×10^{13}	0.756	0.300	6.85×10^5	0.109
	200	2.53	1.01×10^{13}	0.745	0.300	5.47×10^5	0.103
Low-density polyethylene	160	2.09	2.95×10^{10}	0.730	0.194	3.62×10^6	0.125

* Presumptive value from high-density polyethylene

Table 3 Critical apparent shear rate D_c 1/sce

Material	Capillary / Temp. C°	No. 1	No. 2	No. 3	No. 4	No. 5	No. 6
Polypropylene	180	—	5.84×10^2	—	—	—	4.83×10^2
High-density Polyethylene	160	2.30×10^2	—	2.68×10^2	2.40×10^2	2.16×10^2	2.02×10^2
	180	3.20×10^2	—	3.52×10^2	3.36×10^2	2.87×10^2	2.89×10^2
	200	2.87×10^2	—	2.41×10^2	2.78×10^2	3.18×10^2	2.25×10^2

Material	Temperature °C	Capillary	A	B	C	D	E	F	G	H
Low-density polyethylene	160	Refracted point of flow curve	50	35	60	50	55	50	90	120
		Observational value	32~53	16~36	39~94	35~91	35~59	30~52	44~104	69~159
		Value used calculation (mean value of observation)	42.5	26.0	66.5	63.0	49.0	41.0	74.0	114.0

(A.B. Metzner et al.[7])

Table 4 R_e* and N_E/κ^α

Material	Polypropylene		High-density polyethylene						Low-denstity polyethylene		
Temperature °C	180		160		180		200		160		
Capillary	R_e*	N_E/κ^α	R_e*	N_E/κ^α	R_e*	N_E/κ^α	R_e*	N_E/κ^α	Capillary	R_e*	N_E/κ^α
No. 1	—	—	1.88×10^{-5}	6.57×10	3.57×10^{-5}	6.75×10	3.27×10^{-5}	5.51×10	A	1.77×10^{-6}	8.34×10
No. 2	1.13×10^{-4}	8.35×10	—	—	—	—	—	—	B	2.08×10^{-7}	7.93×10
No. 3	—	—	9.61×10^{-5}	6.37×10	1.67×10^{-4}	6.40×10	1.27×10^{-4}	4.88×10	C	3.49×10^{-6}	6.97×10
No. 4	—	—	1.81×10^{-6}	5.72×10	3.48×10^{-6}	6.02×10	2.79×10^{-6}	4.84×10	D	1.15×10^{-5}	6.88×10
No. 5	—	—	1.70×10^{-5}	5.38×10	3.01×10^{-5}	5.59×10	3.85×10^{-5}	4.94×10	E	3.23×10^{-6}	6.81×10
No. 6	2.07×10^{-5}	6.66×10	3.74×10^{-6}	5.01×10	7.56×10^{-6}	5.38×10	5.51×10^{-6}	4.28×10	F	4.16×10^{-7}	6.73×10
									G	4.11×10^{-6}	6.40×10
									H	1.96×10^{-6}	6.27×10

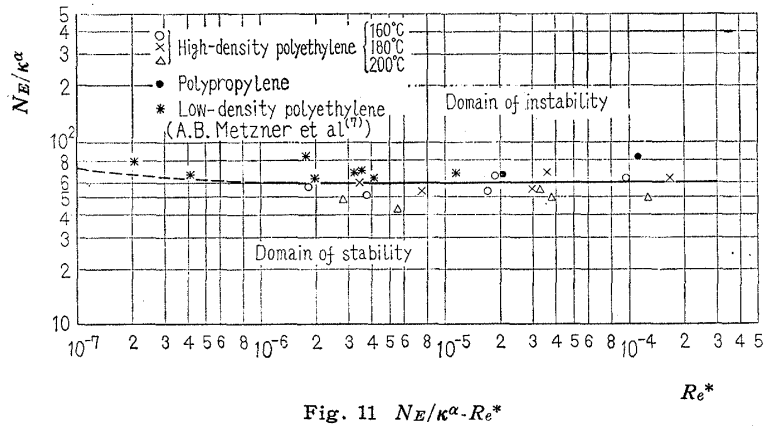

Fig. 11 N_E/κ^α-Re^*

As the assumption is included in the estimation of α and κ^α is not confirmed, the values of N_E/κ^α may fluctuate, but it may be practically useful to be able to estimate from Fig. 11 the critical velocity at which irregular phenomena begin.

6. Conclusion

In the first place, the relation between the extruding pressure and the flow rate in the case of extrusion of the viscoelastic fluid such as molten high polymers through a fixed orifice is found. Moreover, considering the various factors governing the viscoelastic fluid flow, it is found that the flow states depend on two dimensionless numbers R_e^* and N_E. Thus, using these dimensionless numbers, the onset of instabilities of molten high polymers may approximately be determined, and it is verified by the experiments. These results may practically be used to estimate the critical flow rate.

The authors express their cordial thanks to Prof. S. Itaya, Department of Mechanical Engineering, Tokyo Institute of Technology, for his kind advice, and also to Prof. A. B. Metzner, Department of Chemical Engineering, University of Delaware, U. S. A., for his useful suggestions and valuable data offered.

References

(1) J.P. Tordella: *Jour. Appl. Phys.*, Vol. 27 (1956), p. 254.
(2) A.B.Metzner: *Indust. Engng. Chem.*, Vol.50 (1958), p. 1557; Vol. 51 (1959), p. 714.
(3) R.F. Westover and B. Maxwell: *S.P.E.J.*, Vol.13 (1957), p. 13.
(4) J.P. Tordella: *Rheologica Acta*, Vol.1 (1958), p. 216.
(5) R.S. Spencer and R.E. Dillon: *Jour. Colloid Sci.*, Vol. 4 (1949), p. 241.
(6) W. Philippoff: *Trans. Soc. Rheology*, Vol.1 (1957), p. 95.
(7) A.B. Metzner, E.L. Carley and I.K. Park: *Mod. Plast.*, Vol. 38 (1960), P. 133.
(8) R.S. Spencer: *Jour. Polymer Sci.*, Vol. 51 (1950), p. 591.
(9) P.L. Clegg: *Rheology of Elastmers*, (1958), p.174, Pergemon Press, London.
(10) Y. Tomita: *Bulletin of JSME*, Vol.5, No.19 (1962), p. 443.
(11) T. Kotaka, M. Kurata and M. Tamura: *Jour. Appl. Phys.*, Vol.30 (1959), p. 1705.
(12) B.H. Maddock: *Plastics Engng. Jour.*, Vol.15(1959), p. 383.
(13) B.H. Maddock: *Plastics Tech.*, Vol.6 (1960), p. 41.
(14) Y. Tomita: *Trans. Japan Soc. Mech.Engrs.*, Vol. 25, No. 157 (1959), p. 938.
(15) E.B. Bagley and A.M. Birks: *Jour. Appl. Phys.*, Vol. 31 (1960), p. 556.
(16) I.K. Park: *B. Ch. Engineering thesis*, University of Delaware, (1959).